Modelling the effects of fire and rainfall regimes on extreme erosion events in forested landscapes

Owen D Jones[1,2], Petter Nyman[2,3] and Gary J Sheridan[2,3]

[1]The University of Melbourne, Department of Mathematics and Statistics, Melbourne, Australia
[2]The Bushfire Cooperative Research Centre, The University of Melbourne, Melbourne, Australia
[3]The University of Melbourne, Department of Forest and Ecosystem Science, Melbourne, Australia

Corresponding author:
Petter Nyman,
Department of Forest and Ecosystem Science,
The University of Melbourne,
221 Bouverie St, Parkville, Victoria 3010, Australia.
Email: nymanp@unimelb.edu.au
Phone: +61 0408584676

Abstract

Existing models of post-fire erosion have focused primarily on using empirical or deterministic approaches to predict the magnitude of response from catchments given some initial rainfall and burn conditions. These models are concerned with reducing uncertainties associated with hydro-geomorphic transfer processes and typically operate at event timescales. There have been relatively few attempts at modelling the stochastic interplay between fire disturbance and rainfall as factors which determine the frequency and severity with which catchments are conditioned (or primed) for a hazardous event. This process is sensitive to non-stationarity in fire and rainfall regime parameters and therefore suitable for evaluating the effects of climate change and strategic fire management on hydro-geomorphic hazards from burnt areas. In this paper we ask the question, "What is the first-order effect of climate change on the interaction between fires and storms?" The aim is to isolate the effects of fire and rainfall regimes on the frequency of extreme erosion events. Fire disturbance and storms are represented as independent stochastic processes with properties of spatial extent, temporal duration, and frequency of occurrence, and used in a germ-grain model to quantify the annual area affected by extreme erosion events due to the intersection of fire disturbance and storms. The model indicates that the frequency of extreme erosion events will increase as a result of climate change, although regions with frequent storms were most sensitive.

Keywords: wildfire; fire regime; rainfall regime; erosion; debris flow; climate change

1. Introduction

Changes to catchment properties by wildfire can result in increased likelihood of hydro-geomorphic events such as debris flows and flash floods. These events can represent a hazard to water supply systems (Smith et al., 2011), infrastructure (Cannon and Gartner, 2005) and aquatic ecosystems (Bisson et al., 2003). The risk (or probability and severity of consequence) associated with post-fire hydro-geomorphic events depends on the vulnerability of assets in relation to the frequency and magnitude with which hazardous events occur. The hazard (frequency and magnitude of events) is a function of the fire regime, the rainfall regime and their interaction with the landscape (Nyman et al, 2013). While the frequency and magnitude relation is important from a hazards perspective, it is also key to understanding long term erosion rates in forested systems (Kirchner et al., 2001, Meyer et al., 2001, Pierce et al., 2004).

A general distinction can be made between model structures which predict magnitude of response and those that predict the frequency of response (Nyman et al, 2013). Model structures that predict event magnitude after a wildfire are concerned with how rainfall on burnt catchments translates to a response and use information on fire severity, the landscape, and rainfall conditions to predict the magnitude of some response variable (Robichaud et al., 2007, Cannon et al., 2010, Moody, 2012) . Model structures that are designed predict event frequency on the other hand are concerned with the frequency and intensity with which fire and rainfall overlap with the landscape in space and time (Benda and Dunne, 1997, Istanbulluoglu et al., 2004). The two modelling components (frequency versus magnitude) represent different challenges in terms of how model uncertainties are incorporated. In predictions of event magnitude, the response models are usually deterministic and aim to *reduce* uncertainties associated with hydrological transfer processes. In models of event frequency the challenge is to *incorporate* the uncertainties as to what may or may not happen through a probabilistic approach.

The scope of existing modelling tools has been driven largely by the need for understanding post-fire hydro-geomorphic processes and predicting events in a given area *after* a fire has occurred (i.e. the catchment conditions and the fire event are given). At this temporal scale there is a "window of risk" (Prosser and Williams, 1998) for several years within which severe erosion events may occur, depending on whether a storm event of sufficient magnitude occurs within the burnt areas. When a storm does occur in a burnt area, the magnitude of the erosion event is determined through response models which are dependent on many factors including soil properties, topography, and fire impact (the departure from background conditions). Models that quantify hazards during a "window of risk" are by definition restricted to within-burn time scales and not designed to represent both fire and rainfall regimes as variable and non-stationary components of risk. However, both fire and rainfall regimes vary spatially and are sensitive to changing climate (Groisman et al., 1999, Hennessy et al., 2005, Lynch et al., 2007, Bradstock et al., 2009, Flannigan et al., 2009, Williams et al., 2009, Brown et al., 2010) and furthermore, fire regimes can be modified directly through fuel management and suppression (Cary et al., 2009, Price and Bradstock, 2011). Predicting the geomorphic and hydrological response of forested systems to such changes in landscape processes is important for understanding disturbance regimes and geomorphic processes in forested catchments (Dale et al., 2001, Istanbulluoglu et al., 2004).

Predicting the frequency and magnitude of events under variable fire and rainfall regimes involves capturing the nature of the interaction between the causes of risk: fires and rainfall events. The physical modelling of fires, rainfall and subsequent erosion events is potentially a very complex undertaking, requiring detailed deterministic fire and erosion models with many parameters and time-series of forcing inputs. Application of this modelling approach across landscapes is constrained by the availability of the high-resolution data required to fit the models. The deterministic representation of fire and erosion processes can result in very high epistemic uncertainties, due to the large number parameters and modelling steps. These uncertainties in turn can obscure the effects of key elements within the system, such as the frequency of fire and rainfall events.

In this paper we ask the question, “What is the first-order effect of the interaction between fires and storms?” When assessing changes in risk as a result of different fire regimes and/or climate change, we argue that the most important property of the system is the “volume” of the intersection in space and time of burnt areas and storms. The modelling focus should therefore be directed at the *overlap* between fire and storm events, rather than at the geophysical processes that drive them individually. We propose a novel method to quantify the size of this intersection as a function of the regional fire regime and the local rainfall properties. We then apply the model to SE Australia to illustrate how parameters can be obtained from readily available data on fire and rainfall regimes**.**

2. Coverage model (derivation and general definition)

2.1 Coverage Model

We view burn impacts and rain storms as spatial-temporal processes which can be described in terms of their rate of occurrence, their duration and their area. Erosion events in forests occur when rain storms overlap with burnt areas (Fig. 1). The actual magnitude of these erosion events depends on the intensity of rainfall and the susceptibility of the landscape to erosion. In this paper we develop a coverage model which quantifies the size of the intersection between burned areas and storm events that exceed some threshold for a particular response, assuming that the size of the intersection is related to the degree with which the landscape is primed for particular response. The intensity and duration of rain storms are defined for a particular landscape based on rainfall thresholds associated with a pre-defined erosion response. For runoff-generated debris flows after wildfire in western US, for instance, the 30-minute rainfall intensity threshold has been found to vary between 10 and 30 mm h^{-1}(Wells, 1987;Cannon et al, 2001a, Cannon et al, 2008).

<<<<<<<<<<<<<<Fig. 1 here >>>>>>>>>>>>>>>

The term coverage process refers to any stochastic process consisting of a number of sets, usually in some Euclidean space $\mathbb{R}^d$, where we are interested in the volume of some fixed set Ω which is covered by these random sets. A particular type of coverage process is the germ-grain model, in which the random sets are generated by taking a Poisson process (the germs) and then at each point centering independent and identically distributed (or iid) random sets (the grains). Our model uses two independent germ-grain processes, one for storms and the other for fires. Our space will be $\mathbb{R}^3$, where the first two dimensions are space (km^2) and the third is time (*years*). The set Ω represents the catchment for a single year, and we are interested in the "risk set"

$$R = \Omega \cap \text{burnt area} \times \text{duration} \cap \text{stormy area} \times \text{duration} \quad (1)$$

Here R has dimensions $km^2 \times years$. Our fire process will model fire events as patches of disturbance, and our storm process will model high-intensity storm cells, the combination of which is known to have the potential to cause high-magnitude erosion events. Here the duration of a burn impact is the time it takes for the vegetation to recover (a year), rather than the time the fire is active (a couple of days), so the fire duration is really the fire recovery time. Thus we can interpret the volume of R, that is $||R||$, as the erosion hazard due to the overlap between storms and burnt areas. As an example of two independent and overlapping germ-grain processes we simulated fire and storm events over 50 years and show a single realisation of these random processes in a 1000 × 1000 km area (Fig. 2).

<<<<<<<<<<<<<<<Fig. 2 here>>>>>>>>>>>>>>>>

We need some notation to describe storm and fire processes

λ = fire event rate (*km*$^{-2}$ *year*$^{-1}$)

μ = storm event rate (*km*$^{-2}$ *year*$^{-1}$)

α = E||fire event|| (*km*^{2} × *years*)

β = E||rainfall event|| (*km*^{2} × *years*)

Given these definitions, our main result for this section is that

$$\mathrm{E}\|R\| = \|\Omega\|(1 - e^{-\lambda\alpha})(1 - e^{-\mu\beta}). \quad (2)$$

This formula is an analytic solution to the germ and grain process which calculates the size of the spatial and temporal overlap of burnt areas and rain storms using information on the size, duration and frequency of fire and storms. Note that this formula only requires the expected size and rate of fires and storms, and does not depend on their shape. We will use this result to explore the impact of changing burn and storm properties on high-magnitude erosion events.

It is also possible to say something about how variable R is. Let A be a typical fire event centered at the origin, and B a typical storm event centered at the origin (recall that we model fire and storm events as iid sequences). Define $\alpha(x) = \mathrm{E}||(x + A) \cap A||$ and $\beta(x) = \mathrm{E}||(x + B) \cap B||$, where $x + A$ is just the set obtained by adding x to each element of A. Note that while $\alpha = \alpha(0) = \mathrm{E}||A||$ does not depend on the shape of A, $\alpha(x)$ does when $x \neq 0$. We have

$$\begin{aligned}\mathrm{Var}\|R\| &= \int_\Omega\int_\Omega \big((1-e^{-\lambda\alpha(0)})^2 e^{-2\mu\beta(0)}(e^{\mu\beta(x-y)}-1) \\ &\quad +(1-e^{-\mu\beta(0)})^2 e^{-2\lambda\alpha(0)}(e^{\lambda\alpha(x-y)}-1) \\ &\quad +e^{-2(\lambda\alpha(0)+\mu\beta(0))}(e^{\lambda\alpha(x-y)}-1)(e^{\mu\beta(x-y)}-1)\big)\,dx\,dy.\end{aligned} \tag{3}$$

A measure of variation in R is useful if the variation from year to year is important. For instance, large variation in R, would mean that the coincidence of burnt areas and rain storms can be expected to be highly variable between years. Proofs for these results appear in the appendix.

Before we consider the problem of estimating λ, μ, α and β, it is worth collating the assumptions inherent in our model, and some of their implications.

2.2 Model assumptions

1. Burnt areas and rainfall events are independent of each other
2. The size/shape of burnt areas and storms are iid
3. Burn impacts and storms are uniformly distributed in space
4. The rate at which fire and storm events occur is constant

For *Assumption 1* we need to consider dependence in time and space. At the time scale of the model, temporal independence between fires and storms is reasonable. While the fire is actually burning it may affect local precipitation, but this is only a short term effect compared to the time for which burnt landscape is susceptible to erosion events. Perhaps more important is dependence caused by the geography, which will effect patterns of burning and precipitation. This dependence will effect the shape of fires and storms (grains) as the degree of burning or intensity of rainfall may be different upslope or downslope, for example. That is, local geography could affect the intersections of fires and storms. Practically, ignoring such affects means that our risk measure, $\mathrm{E}||R||$, could also have a local component, in that the rate at which risk is converted to actual erosion events depends on the type of landscape the catchment is situated in.

Assumption 2 is saying that the local geography is homogenous across the catchment, so that the shapes of burn areas or storms are statistically similar from one end to the other. Independence of the grains also means that burn areas/storms do not interact if they overlap in space and time.

Assumption 3 is saying that fires and storms are equally likely across the catchment. There will be large scale (germ) effects on the location of fires (more frequent in mountainous areas, for example) and storms (regional weather patterns). By ignoring these effects we are assuming that the catchment area is topographically homogenous (which is not to say flat, but the same type throughout) and with similar weather/vegetation patterns throughout. This means that our fitted model parameters will be specific for the type of catchment being modeled.

Assumption 4 is about seasonality. That is, we are supposing that there are no seasonal patterns in fire and storm events. This is clearly not the case, but we argue that the model will still give useful results. The reason is that burnt areas remain susceptible to erosion events for a long period of time: a year or more. Thus, even though there will be seasonal patterns to fires, storms and high-magnitude erosion events, we can in effect spread them out over the year. The practical implication is that we need to ensure that the rates we use for fires and storms are annual rates.

2.3 Rate at which sediment is generated by debris flows

The effects of wildfire on runoff and sediment availability can result in increased susceptibility to extreme erosion processes such as runoff generated debris flows (Cannon, 2001b, Nyman et al., 2011, García-Ruiz et al., 2012). In forested systems wildfire can therefore operate as a control on the delivery of sediments from headwaters to valley-bottoms and streams (Istanbulluoglu et al., 2004). Predicting the frequency of post-fire debris flows is therefore important for understanding stream processes and sediment dynamics in upland areas. Let ρ be the rate at which the coincidence of storms and burnt areas resulted in debris flows (from Assumption 1 above we imagine that this will dependent of the type of landscape in which the catchment is situated), and let M be the mean sediment yield from debris flows (*Mg km*$^{-2}$). Given $\mathrm{E}\|R\|$, the expected size of the risk set, if we knew ρ and M , then the product of these three, that is $\mathrm{E}\|R\|\rho M$, would give the average annual yield of sediment delivered from post-fire debris flows. The sediment yield per unit area from runoff generated debris flows in Victorian uplands has been measured, and ranges from 1.20×10^4 *Mg km*$^{-2}$ to 2.70×10^4 *Mg km*$^{-2}$ (mean = 1.8×10^4 *Mg km*$^{-2}$) (Nyman et al., 2011). It is convenient to divide $\mathrm{E}\|R\|$ by $\|\Omega\|$, or equivalently to set the volume of the catchment Ω to 1. If we assume transport limited conditions this means that the model output is equal to the annual average mass of sediment generated per unit vulnerable area. The rate ρ can in principle also be estimated, however if, as here, we are only interested in how the sediment delivery will change in response to changing fire and rainfall regimes, then it is sufficient to consider $\mathrm{E}\|R\|M$.

3. Parameter estimation

3.1 Runoff-generated debris flows

We adopt a threshold-based approach to modelling the sediment debris flow response from forests burnt by wildfire. Recent studies have found the initiation of runoff-generated debris flows to be most sensitive to peak rainfall intensities at relatively short timescales (< 0.5 *hours*) (Kean et al., 2011, Staley et al., 2012). Debris flows in the eastern Victorian uplands are triggered by rainfall events with half hour rainfall intensity of at least 35 *mm h*$^{-1}$ (Nyman et al., 2011). Note that, with reference to Assumption 1 and the definition of ρ above, this threshold approach to the rainfall means that we are *only* considering storms which can produce debris flows, at least in our landscape of interest. The chosen threshold thus implicitly incorporates understanding of the rate at which the coincidence of storms and burnt areas results in debris flows, and we thus expect to have $\rho \approx 1$. Catchments are most vulnerable to erosion immediately following burning, and in southeast Australia post-fire debris flows have been observed only during the first year following wildfire. We therefore set the duration of wildfire impact (window of disturbance) to one year.

3.2 Rainfall

From the above considerations, we restrict our attention to short intense storm cells, of duration 0.5 hours and intensity at least 35 *mm* h^{-1}. Such storm cells tend to be small, so we take them to have an area of 10 km^2. This gives $\beta = 10 \times \frac{0.5}{24 \times 365} km^2 years^{-1}$. Storms of this size and duration occur at different frequencies depending on the local rainfall regime. A local rainfall regime is typically described in terms of the intensity-frequency-duration (IFD) curve and the depth-area-reduction factor (DARF). Both are statistical descriptions of rainfall which have been obtained from historical rainfall records. The following section describes how the IFD curve and DARF are used to calculate the rate at which rain storms of a given size and duration appear in the landscape.

To calculate μ we used data from the Australian Bureau of Meteorology (BoM). Let $r(t, x, y)$ be the rainfall intensity at time t and spatial co-ordinates (x, y), and define, for duration h (in $years$) and area A,

$$\begin{aligned} R_k(h; x, y) &= h^{-1} \int_{kh}^{(k+1)h} r(s, x, y) ds \\ \bar{R}_k(h; A) &= \|A\|^{-1} \int \int_A R_k(h; x, y) dx\, dy \end{aligned} \qquad (4)$$

That is, $R_k(h; x, y)$ is the average rainfall intensity at (x, y) over the time period $(kh, (k+1)h)$, and $\bar{R}_k(h; A)$ is the rainfall intensity averaged over the time period $(kh, (k+1)h)$ and over the area A. Note that here $\|A\|$ is the area of A, rather than the volume. Let $R(h; x, y)$ and $\bar{R}(h; A)$ denote randomly sampled values of $R_k(h; x, y)$ and $\bar{R}_k(h; A)$. Let f be a frequency (in $years$), and A an area centered at (x, y), then the functions ϕ and ξ are defined by

$$\begin{aligned} \mathrm{P}(R(h; x, y) > \phi(h, f; x, y)) &= h/f \\ \mathrm{P}(R(h; A) > \phi(h, f; x, y)\xi(\|A\|; x, y)) &= h/f \end{aligned} \qquad (5)$$

We call ϕ a rainfall intensity-frequency-duration (IFD) curve and ξ is called a depth-area-reduction factor (DARF) (Fig. 3a). Note that we will generally drop the x, y from R, ϕ and ξ, where it is unambiguous to do so. From Fig. 3a we see that the depth area reduction factor is $\xi(10) = 0.95$ for storm areas of $\|A\|$ = 10 km^2. Storm duration h has been fixed at 0.5 *hours*, that is $(365 \times 24 \times 2)^{-1}\ years$, for storms with intensity > 35 *mm* h^{-1} and area 10 km^2.Thus the frequency of these events, f, satisfies

$$\phi(h = (365 \times 24 \times 2)^{-1}; f)\xi(\|A\| = 10) = 35\, mm\, h^{-1}. \qquad (6)$$

Using IFD data from the Australian Bureau of Meteorology this gives values of *f* ranging from 2.3 to 5.8, for areas in southeast Australia where post-fire debris flows have been recorded **(**Fig. 3b). Given f we get $\mu = 1/(f\|A\|)$, which values are given in Table 1. The method used to obtain the rainfall regime parameters was developed around the availability of rainfall data (IFD and DARF) from existing records. More sophisticated methods for representing spatial temporal properties are available (see Onof et al., 2000, Wheater et al., 2005)) and can be incorporated in future model development.

<<<<<<<<<<<<<<Fig. 3 here>>>>>>>>>>>>>>>
<<<<<<<<<<<<<<Table 1 here>>>>>>>>>>>>>>>

3.3 Current and future wildfire regimes

If you ignore the shapes of grains in a germ-grain model and just look at their size, you get a compound Poisson process, and these can be found in the literature as fire models (Podur et al., 2010). We use historical fire data from Victoria and Australian Capital Territory to test the assumptions underlying the compound Poisson model, and estimate the rate λ and mean size α of fires (Fig. 4). The distribution of fire sizes displays power law behavior (Fig. 4a). This suggests a Pareto distribution, though note that two or three parameter Weibull distributions have also been found to fit fire size data (Cui and Perera, 2008). We restricted the fires to those greater than 10 km^2 in size, as smaller fires are usually not intense enough to trigger high-magnitude erosion events. For these fires the average rate of occurrence was 9.41×10^{-5} and 1.85×10^{-4} km^2 $year^{-1}$ for Victoria and the Australian Capital Territory respectively, highlighting the regional difference in fire regimes. Wildfires in the Australian Capital Territory are on average smaller and more frequent than in Victoria. The average size of wildfires > 10 km^2 was 201 km^2 and 67 km^2 for Victoria and the Australian Capital Territory respectively. The interarrival times for fires > 10 km^2 were approximately exponentially distributed (Fig. 4b), supporting the idea that they occur according to a Poisson process.

<<<<<<<<<<<<<<Fig. 4 here>>>>>>>>>>>>>>>

3.4 The effect of climate change on fire frequency

A Forest Fire Danger Index (FFDI), based on meteorological variables of rainfall, evaporation, wind temperature and humidity can be used to predict the effect of climate change on fire regimes (McArthur, 1967, Hennessy et al., 2005, Lucas et al., 2007, Bradstock et al., 2008, Dowdy et al., 2009). Climate change projections for southeast Australia indicate that the average FFDI and the number of days with extreme FFDI values will increase (Hennessy et al., 2005, Lucas et al., 2007). The annual FFDI in the region is expected to increase by 2-10% by 2020 and 5-30% by 2050, while the number of days with very high/extreme FFDI is likely to increase by 4-25% and 15-70% by 2020 and 2050 respectively (Hennessy et al., 2005). The effect of these changes in FFDI on fire regimes in Victoria and the Australian Capital Territory has not yet been quantified. However, in similar Eucalypt forests in the Sydney region Bradstock et al. (2009) used a statistical analysis of fire history data and to show empirically that the probability of large fires (> 10 km^2) may increase by 20-84% as result of the changes to FFDI predicted by Hennessy et al. (2005) for 2050 under different climate change scenarios. Thus in this study we use the range of 20-84% increase in probability of large fires as a basis with which to explore the potential effects of climate change on erosion due to debris flows in burnt forests. The average fire size was kept constant while the event rate λ was adjusted to produce a new fire rate (λ_{cc}) which corresponds to either the lower (20%) or the upper (85%) range of increased ignition probabilities (Table 1). In the next section we use the parameters in Table 1 to explore the relative changes in the intensity of the interaction between rain storms and burnt areas.

4. Model Application

In Section 2.3 we introduced the parameter ρ as the rate at which debris flow opportunities actually result in debris flows. In dry Eucalypt forest of southeast Australia, for the threshold value of rainfall intensity considered in Section 3.1, we expect $\rho \approx 1$. Taking $\rho = 1$ and $M = 1.80 \times 10^4$ *Mg* km^{-2} we can give our model outputs in terms the average long term sediment yield (*Mg* km^{-2} $year^{-1}$) from post-fire debris flows in vulnerable areas. Note that this calculation assumes a transport limited system where sediment produced from a debris flows is independent of the frequency, although with further model development it may be possible to account for sediment infilling between events.

For current fire regimes in Victoria and ACT, the long term yield in the model ranged from 0.5×10^2 to 1.25×10^2 *Mg* km^{-2} $year^{-1}$ (Fig. 5a). These values fall in the same region as background erosion rates of $\approx 1.0 \times 10^2$ *Mg* km^{-2} $year^{-1}$ reported for forests in the region (Smith, 1985, Loughran et al., 2004). The similarity between our modelled long-term erosion rates from post-fire debris flows, and longer term rates of erosion, supports the notion that erosion in forests is low in undisturbed conditions, and that over time the sediment delivery is driven by the episodic events (debris flows) which are captured by the coverage model. The average return interval of debris flows was calculated from $1/\gamma$, where γ is the average long term sediment yield (*Mg* km^{-2} $year^{-1}$) divided by M (the average sediment yield from individual debris flows). The model predicts an average return interval of 144 – 360 years (Fig. 5b) which is within the return interval obtained at Myrtle Creek, Victoria (243 – 342 years) through radiocarbon dating of charcoal fragments in debris flow deposits (Smith et al., 2012) but slightly lower than the values obtained for debris flows in the Cotter Catchments in Australian Capital Territory (410 – 440) (Worthy and Wasson, 2004, Worthy, 2006).

The model indicates that local rainfall regimes may have large impacts on sediment delivery from debris flows. For current fire regimes a 2.1 fold increase in storm event rate from at Kilmore ($\mu = 1.96 \times 10^{-2}$) to Bright ($\mu = 4.27 \times 10^{-2}$) (Table 1) resulted in a similar shift in the amount of sediment delivered from debris flows. However, the strength of the rainfall regime effect (or slope) was dependent on the fire regime, with Victoria being slightly more sensitive to changes in rainfall regimes than ACT. This means that increasing fire frequency due to climate change resulted in increased sensitivity to changes in storm event rates. Or in other words, increasing storm event rates will have large effects on landscape response when fire impacts are more frequent in the landscape. Victoria was more sensitive to changes in fire frequency than the ACT, because of its relatively large average fire size (210 km^{-2} in Victoria compared to 67 km^{-2} in ACT). The model indicates that climate effects on fire frequency could result in a 1.1 to 1.8 fold increase in the average annual erosion rates from debris flows by 2050, with the magnitude of the shift depending on the local rainfall regimes and the average fire size.

<<<<<<<<<<<<<<Fig. 5 here>>>>>>>>>>>>>>>

5. Conclusion

Fire and rainfall processes operate in the landscapes to produce a mosaic with erosion events occurring as "episodic patches of activity" (Miller et al., 2003). Under this description, the patches are determined by intersection between storms and burnt areas, and the activity (erosion processes) is determined by landscape attributes and the sensitivity to fire impacts. If one's aim is to predict the likelihood of water quality impact *following* fire then the modelling effort should focus on activity (erosion processes) and how this changes with different rainfall inputs and fire severities. If the aim is to quantify risk within a catchment in the context of, for example climate change, then the focus should be on the interaction between storms and burnt areas. Separating between these different sources of uncertainty is important when moving towards risk-based approaches in wildfire and forest management (Hyde et al., 2012, Thompson et al, 2011).

In this paper we have shown how coverage processes provide a powerful framework within which the interaction of burnt areas and storms can be quantified. The expected area of intersection $\mathrm{E}\|R\|$ is a measure of event frequency that is independent of the landscape vulnerability and the sediment transfer processes that occur following fire. It represents the average annual area ($km^2 \times years$) where fire and rainfall satisfy the conditions known to be required for high-magnitude erosion events to occur in a particular landscape. Assuming a vulnerable landscape where all these potential erosion events actually occur, and given an estimate of the size of these erosion events, we get the annual average sediment load from the particular processes being considered in the coverage model. Essentially the model output is a function of both the coincidence of burnt areas and storms (patches or intersections) and the vulnerability of the landscape (erosion and sediment transfer processes). Here, we were specifically interested in debris flows in Eucalypt forest of SE Australia and therefore used a known half-hour rainfall threshold for post-fire debris flow initiation as a response threshold. Other thresholds may apply for different environments and processes. The strength of the model is that it responds directly to changes in fire disturbance and rainfall regimes.

Our risk model has a number of applications. To quantify the effect of climate change on the risk of high-magnitude erosion events, we need to quantify the effect of climate change on α, β, λ and μ. In this paper we modelled the effect of climate change on fire frequency (λ) and used this to evaluate climate change effects on erosion regimes in different rainfall regimes. This approach could be extended to include climate change effect on fire-size and storm frequency. Another immediate application of the model is to quantify the effect of planned burns. That is, we consider fires to be either low-impact planned burns or high-impact wildfires, each with their own frequency and size parameters. As we increase the frequency of prescribed burns the frequency of wildfires will reduce (e.g. Bradstock et al., 2012). Provided we can quantify the relative frequencies of prescribed burns and wildfires, we can use the model to quantify the change in the risk of high-magnitude erosion events. By representing the first order effects of fire and rainfall on catchment processes the coverage model is able to capture, with relative few parameters, the key factors that contribute to changes in risk over time.

7. Acknowledgements

The research was carried out with funding from the Bushfire Cooperative Research Centre. Fire and rainfall parameters were obtained using data from Department of Sustainability and Environment and the Australian Bureau of Meteorology. We are also thankful for useful comments and suggestions from the reviewers.

8. Appendix: Germ and grain model

Suppose that we have two independent Boolean models in $\mathbb{R}^k$. That is, let $\{\xi_i\}$ and $\{\zeta_i\}$ be independent stationary Poisson processes with intensities λ_ξ and λ_ζ, and let $\{X_i\}$ and $\{Y_i\}$ be mutually independent i.i.d. sequences of random sets, then our two models are $\mathcal{X} = \{\xi_i + X_i\}$ and $\mathcal{Y} = \{\zeta_i + Y_i\}$. Let Ω be a Borel subset of $\mathbb{R}^k$ then the intersection of Ω, $\mathcal{X}$ and $\mathcal{Y}$ is given by $A = \Omega \cap (\cup_i \xi_i + X_i) \cap (\cup_i \zeta_i + Y_i)$. Let $\|A\|$ denote the content (Lebesgue measure) of A, then we have:

8.1 Proposition

If $\|\Omega\| < \infty$ then $\mathrm{E}\|A\| = \|\Omega\|(1 - e^{-\lambda_\xi \mathrm{E}\|X\|})(1 - e^{-\lambda_\zeta \mathrm{E}\|Y\|})$, where X and Y are random sets, distributed as the X_i and Y_i respectively. Moreover, let $\alpha_X(x) = \mathrm{E}\|(x+X) \cap X\|$ and $\alpha_Y(x) = \mathrm{E}\|(x+Y) \cap Y\|$, then

$$\begin{aligned}\mathrm{Var}\|A\| \;=\; \int_\Omega \int_\Omega \Big(& (1 - e^{-\lambda_\xi \alpha_X(0)})^2 e^{-2\lambda_\zeta \alpha_Y(0)} (e^{\lambda_\zeta \alpha_Y(x-y)} - 1) \\ & + (1 - e^{-\lambda_\zeta \alpha_Y(0)})^2 e^{-2\lambda_\xi \alpha_X(0)} (e^{\lambda_\xi \alpha_X(x-y)} - 1) \\ & + e^{-2(\lambda_\xi \alpha_X(0) + \lambda_\zeta \alpha_Y(0))} (e^{\lambda_\xi \alpha_X(x-y)} - 1)(e^{\lambda_\zeta \alpha_Y(x-y)} - 1)\Big)\, dx\, dy.\end{aligned}$$

8.2 Proof

Let $1_\mathcal{X}(x) = \begin{cases} 1 & x \in \cup_i \xi_i + X_i \\ 0 & \text{otherwise} \end{cases}$, $1_\mathcal{Y}(x) = \begin{cases} 1 & x \in \cup_i \zeta_i + Y_i \\ 0 & \text{otherwise} \end{cases}$, then from Hall [1988] Equation (3.4) we have

$$\begin{aligned}\mathrm{E}\|A\| &= \mathrm{E}\int_\Omega 1_\mathcal{X}(x) 1_\mathcal{Y}(x) dx \;=\; \int_\Omega \mathrm{E}1_\mathcal{X}(x)\mathrm{E}1_\mathcal{Y}(x) dx \\ &= \int_\Omega \mathrm{P}(x \text{ covered by } \mathcal{X})\mathrm{P}(x \text{ covered by } \mathcal{Y}) \;=\; \int_\Omega (1 - e^{-\lambda_\xi \mathrm{E}\|X\|})(1 - e^{-\lambda_\zeta \mathrm{E}\|Y\|}) \\ &= \|\Omega\|(1 - e^{-\lambda_\xi \mathrm{E}\|X\|})(1 - e^{-\lambda_\zeta \mathrm{E}\|Y\|}).\end{aligned}$$

Note that the result still holds when $\mathrm{E}\|X\| = \infty$ or $\mathrm{E}\|Y\| = \infty$.

For the variance we note first that

$$\mathrm{E}\|A\|^2 = \mathrm{E}\int_\Omega 1_\mathcal{X}(x)1_\mathcal{Y}(x)dx \int_\Omega 1_\mathcal{X}(y)1_\mathcal{Y}(y)dy = \int_\Omega\int_\Omega \mathrm{E}1_\mathcal{X}(x)1_\mathcal{X}(y)\mathrm{E}1_\mathcal{Y}(x)1_\mathcal{Y}(y)dx\,dy$$

From Hall (1988) Equation (3.6) and preceding calculations

$$\begin{aligned}\mathrm{E}1_\mathcal{X}(x)1_\mathcal{X}(y) &= \mathrm{P}(x \text{ and } y \text{ covered by } \mathcal{X}) \\ &= 1 - \mathrm{P}(x \text{ not covered by } \mathcal{X}) - \mathrm{P}(y \text{ not covered by } \mathcal{X}) + \mathrm{P}(\text{neither } x \text{ nor } y \text{ covered by } \mathcal{X}) \\ &= 1 - 2e^{-\lambda_\xi \alpha_X(0)} + e^{-2\lambda_\xi \alpha_X(0) + \lambda_\xi \alpha_X(x-y)}\end{aligned}$$

Thus

$$\begin{aligned}\mathrm{Var}\|A\| &= \mathrm{E}\|A\|^2 - (\mathrm{E}\|A\|)^2 \\ &= \int_\Omega\int_\Omega \Big((1 - 2e^{-\lambda_\xi \alpha_X(0)} + e^{-2\lambda_\xi \alpha_X(0) + \lambda_\xi \alpha_X(x-y)})(1 - 2e^{-\lambda_\zeta \alpha_Y(0)} + e^{-2\lambda_\zeta \alpha_Y(0) + \lambda_\zeta \alpha_Y(x-y)}) \\ &\qquad - (1 - e^{-\lambda_\xi \alpha_X(0)})^2 (1 - e^{-\lambda_\zeta \alpha_Y(0)})^2\Big)\, dx\, dy \\ &= \int_\Omega\int_\Omega \Big((1 - e^{-\lambda_\xi \alpha_X(0)})^2 e^{-2\lambda_\zeta \alpha_Y(0)}(e^{\lambda_\zeta \alpha_Y(x-y)} - 1) + (1 - e^{-\lambda_\zeta \alpha_Y(0)})^2 e^{-2\lambda_\xi \alpha_X(0)}(e^{\lambda_\xi \alpha_X(x-y)} - 1) \\ &\qquad + e^{-2(\lambda_\xi \alpha_X(0) + \lambda_\zeta \alpha_Y(0))}(e^{\lambda_\xi \alpha_X(x-y)} - 1)(e^{\lambda_\zeta \alpha_Y(x-y)} - 1)\Big)\, dx\, dy.\end{aligned}$$

9. References

Benda L and Dunne T (1997) Stochastic forcing of sediment supply to channel networks from landsliding and debris flow. Water Resour Res 33: 2849-63. doi:10.1029/97WR02388

Bisson PA, Rieman BE, Luce C, Hessburg PF, Lee DC, Kershner JL et al. (2003) Fire and aquatic ecosystems of the western USA: current knowledge and key questions. Forest Ecol and Manage 178: 213-29. doi:10.1016/S0378-1127(03)00063-X

Bradstock R, Davies I, Price O, and Cary G (2008) Effects of climate change on bushfire threats to biodiversity, ecosystem processes and people in the Sydney region. Climate Change Impacts and Adaptation Research Project 050831. Report to the New South Wales Department of Environment and Climate Change. pp. 72. http://www.environment.nsw.gov.au/resources/climatechange/BushfireReport2008.pdf.

Bradstock RA, Boer MM, Cary GJ, Price OF, Williams RJ, Barrett D et al. (2012) Modelling the potential for prescribed burning to mitigate carbon emissions from wildfires in fire-prone forests of Australia. Int J Wildland Fire 21: 629-39. doi:10.1071/WF11023

Bradstock RA, Cohn JS, Gill AM, Bedward M, and Lucas C (2009) Prediction of the probability of large fires in the Sydney region of south-eastern Australia using fire weather. Int J Wildland Fire 18: 932-43. doi:10.1071/WF08133

Brown JR, Jakob C, and Haynes JM (2010) An evaluation of rainfall frequency and intensity over the Australian region in a global climate model. J Climate 23: 6504-25. doi:10.1175/2010JCLI3571.1

Cannon SH, Kirkham RM, and Parise M (2001a) Wildfire-related debris-flow initiation processes, Storm King Mountain, Colorado. Geomorphology 39: 171-88. doi: 10.1016/S0169-555X(00)00108-2

Cannon SH (2001b) Debris-flow generation from recently burned watersheds. Env & Eng Geosc 7: 321-41. doi:10.2113/gseegeosci.7.4.321

Cannon SH and Gartner JE (2005) Wildfire-related debris flow from a hazards perspective. In Jakob M and Hungr O (eds) Debris-flow Hazards and Related Phenomena. pp. 363-385. Springer Berlin Heidelberg, Berlin

Cannon SH, Gartner JE, Wilson RC, Bowers JC, and Laber JL (2008) Storm rainfall conditions for floods and debris flows from recently burned areas in southwestern Colorado and southern California. Geomorphology 96: 250-69. doi:10.1016/j.geomorph.2007.03.019

Cannon SH, Gartner JE, Rupert MG, Michael JA, Rea AH, and Parrett C (2010) Predicting the probability and volume of postwildfire debris flows in the intermountain western United States. Geol Soc Am Bull 122: 127-44. doi:10.1130/b26459.1

Cary GJ, Flannigan MD, Keane RE, Bradstock RA, Davies ID, Lenihan JM et al. (2009) Relative importance of fuel management, ignition management and weather for area burned: evidence from five landscape–fire–succession models. Int J Wildland Fire 18: 147-56. doi:10.1071/WF07085

Cui W and Perera AH (2008) What do we know about forest fire size distribution, and why is this knowledge useful for forest management? Int J Wildland Fire 17: 234-44. doi:10.1071/WF06145

Dale VH, Joyce LA, McNulty S, Neilson RP, Ayres MP, Flannigan MD et al. (2001) Climate change and forest disturbances. Bioscience 51: 723-34. doi:10.1641/0006-3568(2001)051[0723:CCAFD]2.0.CO;2

Dowdy AJ, Mills GA, Finkele K, and de Groot W (2009) Australian fire weather as represented by the McArthur Forest Fire Danger Index and the Canadian Forest Fire Weather Index. CAWCR Technical Report No. 10. pp. 91. Centre for Australian Weather and Climate Research. http://cawcr.vm.csiro.au/publications/technicalreports/CTR_010.pdf

Flannigan MD, Krawchuk MA, de Groot WJ, Wotton BM, and Gowman LM (2009) Implications of changing climate for global wildland fire. Int J Wildland Fire 18: 483-507. doi:10.1071/WF08187

García-Ruiz JM, Arnáez J, Gómez-Villar A, Ortigosa L, and Lana-Renault N (2012) Fire-related debris flows in the Iberian Range, Spain. Geomorphology: doi:10.1016/j.geomorph.2012.03.032

Groisman PY, Karl TR, Easterling DR, Knight RW, Jamason PF, Hennessy KJ et al. (1999) Changes in the probability of heavy precipitation: Important indicators of climatic change. Climatic Change 42: 243-83. doi:10.1007/978-94-015-9265-9_15

Hennessy K, Lucas C, Nicholls N, J Bathols, Suppiah R, and Ricketts J (2005) Climate change impacts on fire-weather in south-east Australia. pp. 91. CSIRO Marine and Atmospheric Research. Aspendale, Victoria

Hyde K, Dickinson MB, Bohrer G, Calkin D, Evers L, Gilbertson-Day J et al. (2012) Research and development supporting risk-based wildfire effects prediction for fuels and fire management: status and needs. Int Wildland Fire: doi:10.1071/WF11143

Istanbulluoglu E, Tarboton DG, Pack RT, and Luce CH (2004) Modeling of the interactions between forest vegetation, disturbances, and sediment yields. J Geophys Res 109: doi:10.1029/2003JF000041

Kean JW, Staley DM, and Cannon SH (2011) In situ measurements of post-fire debris flows in southern California: Comparisons of the timing and magnitude of 24 debris-flow events with rainfall and soil moisture conditions. J Geophys Res-Earth Surf 116: doi:10.1029/2011jf002005

Kirchner JW, Finkel RC, Riebe CS, Granger DE, Clayton JL, King JG et al. (2001) Mountain erosion over 10 yr, 10 k.y., and 10 m.y. time scales. Geology 29: 591-4. doi:10.1130/0091-7613(2001)029<0591:MEOYKY>2.0.CO;2

Leclerc G and Schaake J (1972) Derivation of hydrologic frequency curves. Report 142. pp. 15. Massachutes Institure of Technology, Cambridge.

Loughran RJ, Elliott GL, McFarlane DJ, and Campbell BL (2004) A Survey of Soil Erosion in Australia using Caesium-137. Austr Geograph Stud 42: 221-33. doi:10.1111/j.1467-8470.2004.00261.x

Lucas C, Hennessy K, Mills G, and Bathols J (2007) Bushfire weaher in southeast Australia: Recent trends and projected climate change impacts. pp. 84. Bushfire Cooperative Research Centre, Melbourne.

Lynch AH, Beringer J, Kershaw P, Marshall A, Mooney S, Tapper N et al. (2007) Using the Paleorecord to Evaluate Climate and Fire Interactions in Australia. Ann Rev Earth and Plan Sci 35: 215-39. doi:10.1146/annurev.earth.35.092006.145055

McArthur AG (1967) In Fire behaviour in eucalypt forests [by] A. G. McArthur. Vol. pp. Forestry and Timber Bureau, Canberra.

Meyer GA, Pierce JL, Wood SH, and Jull AJT (2001) Fire, storms, and erosional events in the Idaho batholith. Hydrol Processes 15: 3025-38. doi:10.1002/hyp.389

Miller D, Luce C, and Benda L (2003) Time, space, and episodicity of physical disturbance in streams. Forest Ecol and Manage 178: 121-40. doi:10.1016/S0378-1127(03)00057-4

Miller J, Frederick R, and Tracey R (1973) Precipitation-frequncy atlas of the western United States. In White R (ed) NOAA Atlas 2. Vol. 2, pp. 48. National Oceanic and Atmospheric Administration, Maryland.

Moody JA (2012) An analytical method for predicting postwildfire peak discharges. In Salzar K and McNutt MK (eds) U.S. Geological Survey Scientific Investigations Report 2011-5236, pp. 1-48, US Geological Survey, Virginia

Nyman P, Sheridan GJ, Smith HG, and Lane PNJ (2011) Evidence of debris flow occurrence after wildfire in upland catchments of south-east Australia. Geomorphology 125: 383-401. doi:10.1016/j.geomorph.2010.10.016

Nyman P, Sheridan GJ, and Lane PN (2013) Hydro-geomorphic response models for burned areas and their applications in land management. Prog. Phys. Geog. 37: 787-812. doi:10.1177/0309133313508802

Onof C, Chandler RE, Kakou A, Northrop P, Wheater HS, and Isham V (2000) Rainfall modelling using Poisson-cluster processes: a review of developments. Stochastic Environ Res And Risk Assesm 14: 384-411. doi:10.1007/s004770000043

Osborn HB, Lane LJ, and Myers VA (1980) Rainfall/watershed relationships for southwestern thunderstorms. Trans ASAE 23: 82-0087.

Pierce JL, Meyer GA, and Jull AJT (2004) Fire-induced erosion and millennialscale climate change in northern ponderosa pine forests. Nature 432: 87-90. doi:10.1038/nature03058

Podur JJ, Martell DL, and Stanford D (2010) A compound Poisson model for the annual area burned by forest fires in the province of Ontario. Environmetrics 21: 457-69. doi:10.1002/env.996

Price OF and Bradstock RA (2011) Quantifying the influence of fuel age and weather on the annual extent of unplanned fires in the Sydney region of Australia. Int J Wildland Fire 20: 142-51. doi:10.1071/wf10016

Prosser IP and Williams L (1998) The effect of wildfire on runoff and erosion in native Eucalyptus forest. Hydrol Processes 12: 251-65. doi:10.1002/(SICI)1099-1085(199802)12:2<251::AID-HYP574>3.0.CO;2-4

Robichaud PR, Elliot WJ, Pierson FB, Hall DE, and Moffet CA (2007) Predicting postfire erosion and mitigation effectiveness with a web-based probabilistic erosion model. Catena 71: 229-41. doi:10.1016/j.catena.2007.03.003

Smith HG, Sheridan GJ, Lane PNJ, Nyman P, and Haydon S (2011) Wildfire effects on water quality in forest catchments: A review with implications for water supply. J Hydrol 396: 170-92. doi:10.1016/j.jhydrol.2010.10.043

Smith HG, Sheridan GJ, Nyman P, Child DP, Lane PNJ, Hotchkis MAC et al. (2012) Quantifying sources of fine sediment supplied to post-fire debris flows using fallout radionuclide tracers. Geomorphology 139–140: 403-15. doi:10.1016/j.geomorph.2011.11.005

Smith JD (1985) Modelling of 210Pb behaviour in the catchment and sediment of Lake Tali Karng, Victoria, and estimation of recent sedimentation rates. Mar and Freshwater Res 36: 15. doi:10.1071/MF9850015

Staley D, Kean J, Cannon S, Schmidt K, and Laber J (2012) Objective definition of rainfall intensity–duration thresholds for the initiation of post-fire debris flows in southern California. Landslides: 1-16. doi:10.1007/s10346-012-0341-9

Thompson M, Calkin D, Finney M, Ager A, and Gilbertson-Day J (2011) Integrated national-scale assessment of wildfire risk to human and ecological values. Stochastic Environ Res And Risk Assesm 25: 761-80. doi:10.1007/s00477-011-0461-0

Wells G (1987) The effects of fire on the generation of debris flows in southern California. Rev. Eng. Geol 7: 105-14.

Wheater H, Chandler R, Onof C, Isham V, Bellone E, Yang C et al. (2005) Spatial-temporal rainfall modelling for flood risk estimation. Stochastic Environ Res And Risk Assesm 19: 403-16. doi:10.1007/s00477-005-0011-8

Williams RJ, Bradstock RA, Cary GJ, Gill AM, Liedloff AC, Lucas C et al. (2009) Interactions between climate change, fire regimes and biodiversity in Australia: a preliminary assessment. pp. 208. Report to the Department of Climate Change. Canberra

Worthy M (2006) Major erosion events and past fires in the Cotter River Catchment. In Cotter Catchment Remediation Project. Centre for resource and environmental studies, Australian National University, Canberra.

Worthy M and Wasson R (2004) Fire as an agent of geomorphic change in southeastern Australia: implications for water quality in the Australian Capital Territory. In Roach ID (ed) Regolith. Vol. pp. 417-418, CRC Landscape Environments and Mineral Exploration, Canberra.

Tables

Table 1. Storm and fire regime parameters for debris flow prone regions in southeast Australia.

Location	Catchment area	Storm event rate [a]	Storm size	Fire event rate	Fire size	Fire event rate with climate change (2050)[b]
		$\times10^{-2}$	$\times10^{-4}$	$\times10^{-4}$		$\times10^{-4}$
	$\|\Omega\|$	μ	β	λ	α	λ_{cc}
	km^2* years	km^{-2} $year^{-1}$	km^2 *year	km^{-2} $year^{-1}$	km^2 *year	km^{-2} $year^{-1}$
Victoria						
Licola		3.20				
Bright	1	4.27	5.7	0.941	201	1.13 – 1.74
Kilmore		1.96				
Australian Capital Territory						
Namadgi NP	1	2.85	5.7	1.850	67	2.22 – 3.42

[a] Based on intensity-frequency-duration coefficients from Australian Bureau of Meteorology.

[b] Parameters for climate change scenarios obtained based on predictions in Hennessy et al. (2005) and Bradstock et al. (2009).

Figures

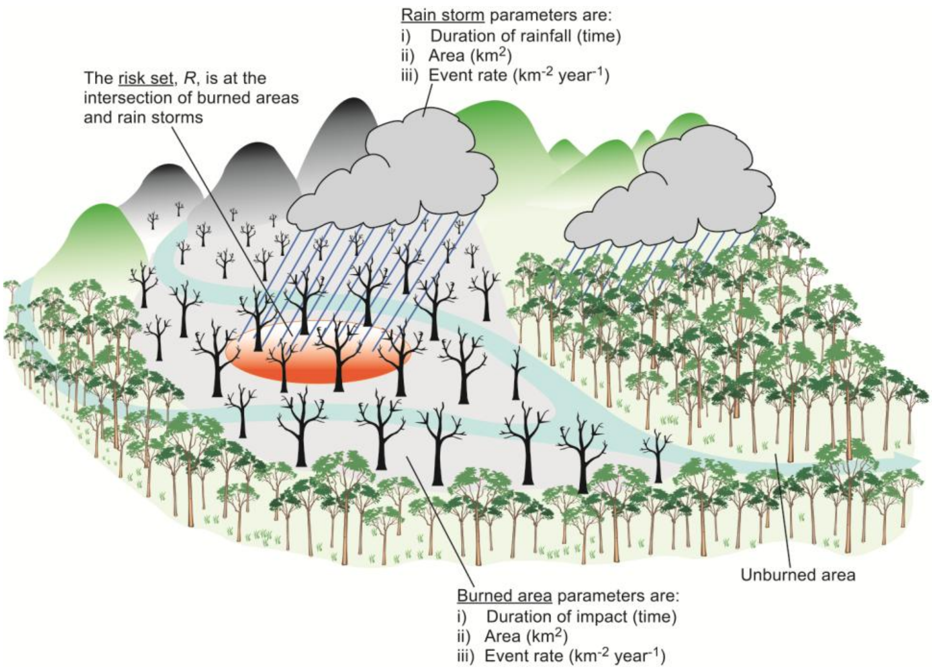

Fig. 1. The model is focused on quantifying the size of the intersection between storm events and burnt areas. The size of this area, or the risk set *R*, is proportional to the rate at which sediment is being produced from erosion events, which are defined by landscape-specific rainfall thresholds associated with a particular response, such as flash floods or debris flows.

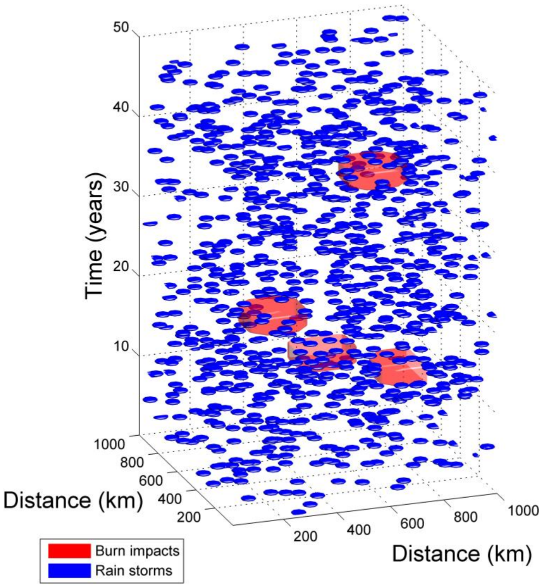

Fig.2. A single realisation of rain storms and burn impacts in space (1000 km x 1000 km) and time (50 years). For burn impacts in this hypothetical scenario the mean radius of the disc shaped burn areas is 100 km, the duration of impact is 2 years and the average return interval for wildfires is 20 years. The corresponding values for rain storms are 1 km, 30 minutes and 2 years. The risk set, *R*, where rain storm and burn impacts overlap, is where extreme erosion events may occur.

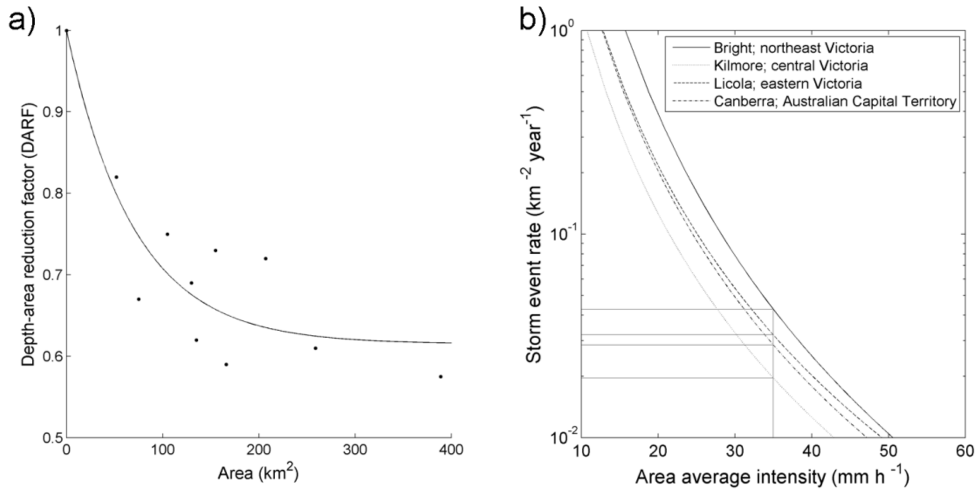

Fig. 3. a) Fixed area depth area reduction factor (DARF) for half hour rainfall fitted using equation by Leclerc and Schaake (Leclerc and Schaake, 1972) and data from Miller et al. (Miller et al., 1973) and Osborn et al. (Osborn et al., 1980). b) Storm event rate (μ; km^{-2} $year^{-1}$) at four locations in southeast Australia as a function of spatially averaged half-hour rainfall intensity for a storm area of 10 km^2.

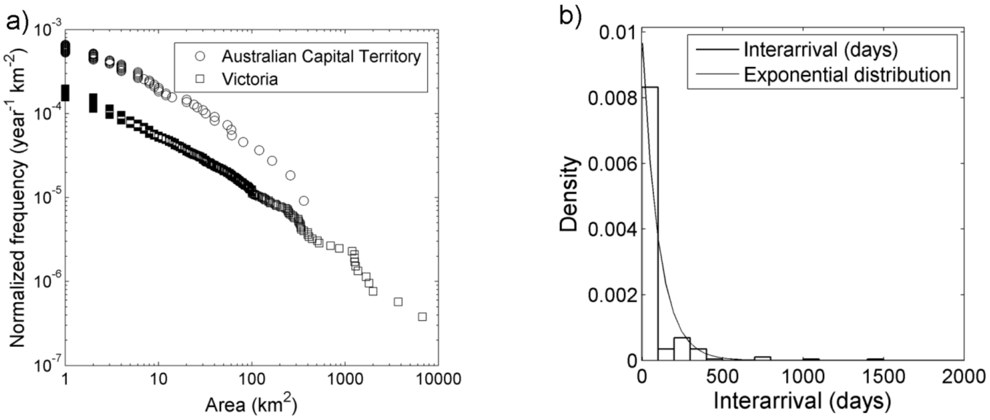

Fig. 4. a) The fire size-frequency distribution for wildfire in Victoria (VIC) (1972-2009) and Australian Capital Territory (ACT) (1936-1999). b) Inter-arrival time distributions for 1040 fires > 10 km^2 in Victoria and ACT.

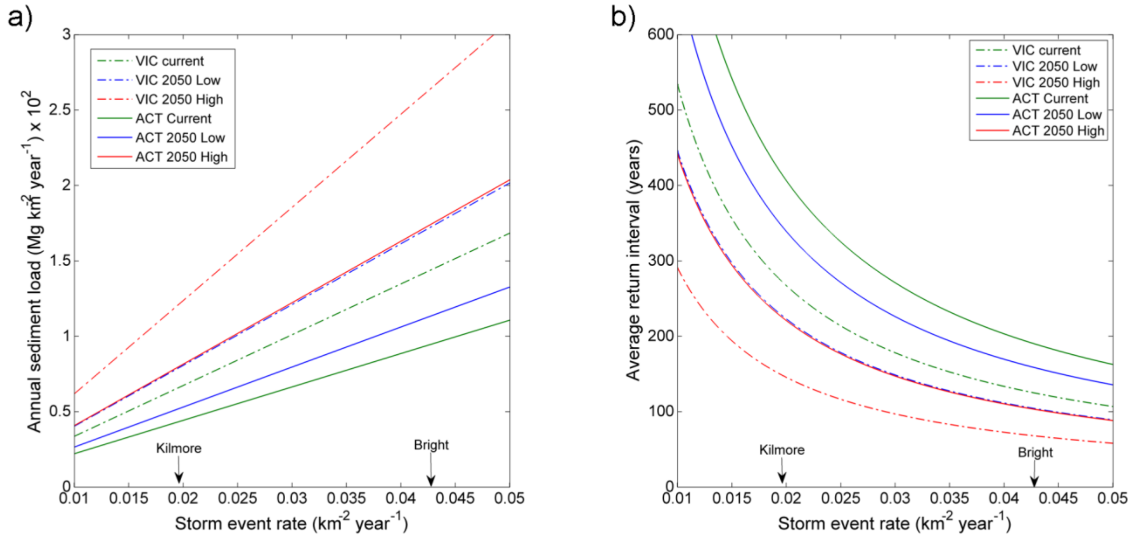

Fig. 5. a) Annual average sediment load and b) average return interval for runoff generated debris flows in susceptible catchments of burnt areas in southeast Australia as a function of storm event rates and for current and future wildfire regimes. The model uses 30-minute rainfall intensity (I_{30}) of 35 mm h^{-1} as a threshold for debris flow initiation. Rainfall threshold and event-based sediment loads were obtained from Nyman et al (2011). High and low climate change impacts correspond with lower and upper bounds of the range of impacts from Bradstock et al. (2009).

University Library

MINERVA ACCESS

A gateway to Melbourne's research publications

Minerva Access is the Institutional Repository of The University of Melbourne

Author/s:
Jones, OD; Nyman, P; Sheridan, GJ

Title:
Modelling the effects of fire and rainfall regimes on extreme erosion events in forested landscapes

Date:
2014-12-01

Citation:
Jones, O. D., Nyman, P. & Sheridan, G. J. (2014). Modelling the effects of fire and rainfall regimes on extreme erosion events in forested landscapes. STOCHASTIC ENVIRONMENTAL RESEARCH AND RISK ASSESSMENT, 28 (8), pp.2015-2025. https://doi.org/10.1007/s00477-014-0891-6.

Persistent Link:
http://hdl.handle.net/11343/282894

File Description:
Accepted version